ADVANCING EARTH AND SPACE SCIENCES

AGU

Geophysical Research Letters®

Key Points:

- The diurnal temperature range (DTR) has a local minimum near average temperatures of 0°C
- DTR in observations shrinks strongly for average temperatures below 0°C and expands for warmer temperatures
- Climate models that reproduce the local DTR minimum near 0°C show a significant slowdown of DTR shrinking in recent decades

Diurnal Temperature Range Trends Differ Below and Above the Melting Point

Felix Pithan[1] [ORCID] and Leonhard Schatt[1,2]

[1]Helmholtz Centre for Polar and Marine Research, Alfred Wegener Institute, Bremerhaven, Germany, [2]University of Bayreuth, Bayreuth, Germany

Abstract The globally averaged diurnal temperature range (DTR) has shrunk since the mid-20th century, and climate models project further shrinking. Observations indicate a slowdown or reversal of this trend in recent decades. Here, we show that DTR has a minimum for average temperatures close to 0°C. Observed DTR shrinks strongly at colder temperature, where warming shifts the average temperature toward the DTR minimum, and expands at warmer temperature, where warming shifts the average temperature away from the DTR minimum. Most, but not all climate models reproduce the minimum DTR close to average temperatures of 0°C and a stronger DTR shrinking at colder temperature. In models that reproduce the DTR minimum, DTR shrinking slows down significantly in recent decades. Models project that the global-mean DTR will shrink over the 21st century, and models with a DTR minimum close to 0°C project slower shrinking than other models.

Plain Language Summary The diurnal temperature range, that is, the difference between daily maximum and minimum temperatures, affects both human health and plant development. Global data sets have shown a shrinking diurnal temperature range since the 1950s, but a recent study found that the diurnal temperature range had expanded again. In this study, we investigate how the diurnal temperature range behaves at different mean temperatures. We find that the diurnal temperature range is particularly small for temperatures close to the melting point of water (0°C), and larger for both colder and warmer temperatures. Due to the latent heat of freezing/melting, more energy is required to warm the soil from −1 to +1°C than from −3 to −1°C or from 1 to 3°C. The diurnal temperature range shrinks in regions and seasons with negative average temperature, where global warming pushes the average closer to 0°C and expands for warmer temperature. Most, but not all climate models also show a narrow diurnal temperature range near 0°C, shrinking of the temperature range at colder temperature and a slower reduction in the diurnal temperature range in recent decades. Models suggest that the currently observed expansion of the diurnal temperature range is a transient phenomenon.

1. Introduction

The diurnal temperature range (DTR), or difference between daily minimum and maximum temperature, is an important climate indicator (Braganza et al., 2004) with substantial effects on human health (Cheng et al., 2014) and crop yields (Lobell, 2007). The global-mean DTR over land areas has decreased over the second half of the 20th century, in particular between 1960 and 1980 (Gulev et al., 2021). Some areas, mostly in the midlatitudes, have experienced positive DTR trends. Huang et al. (2023) recently reported that the global trend had reversed, and DTR over global land areas had increased between 1980 and 2021.

Changes in the DTR have been attributed to changes in cloud cover (Dai et al., 1997, 1999; Doan et al., 2022; Zhong et al., 2023), with increases in cloud cover dampening both daytime warming from incoming solar radiation and nighttime longwave radiative cooling. Observed decreases ("solar dimming" until about 1980) and increases ("solar brightening" since about 1980 over Europe and 2005 over China) of incoming solar radiation at the surface (Schwarz et al., 2020) particularly affect daily maximum temperature and thus DTR. These changes in incoming solar radiation at the surface are partly attributed to air pollution. Land-surface feedbacks such as increased heating of dry soils during droughts and heatwaves further affect maximum temperatures and the DTR (Daramola et al., 2024; Zhou et al., 2009), whereas temperature feedbacks in the stable boundary layer particularly affect nighttime temperatures (Walters et al., 2007).

Lindvall and Svensson (2015) found that climate models of the 5th coupled model intercomparison project (CMIP5) mostly underestimated the DTR compared to observations. Most models agreed on an overall decrease in DTR over the historical period and in future projections with continued increases in greenhouse gas

concentrations. CMIP6 models also tend to underestimate DTR and project further decreases for the 21st century, except under the low-emission scenario SSP1-2.6 (Wang et al., 2024).

Many studies have addressed DTR trends in individual regions, or compared regional trends across the globe. Mid-latitude DTR has a minimum for mean temperatures close to 0°C in climate model output analyzed by Stone and Weaver (2003), and whether such a melting-point effect can be seen in observations and affects DTR trends has yet to be understood. In this paper, we test the hypotheses that (a) the DTR is small (has a relative minimum) close to the freezing/melting point of water, where the latent heat release or uptake during the phase transition dampens temperature fluctuations, and (b) this relative minimum in DTR affects DTR trends, which are more negative below than above 0°C.

2. Data

2.1. Station Observations

We use station observations of surface air temperature measured 2 m above the ground from the Neumayer research station (Wesche et al., 2016) in Antarctica (1983–2022) and the AWIPEV research base in Ny Ålesund, Svalbard (1994–2022). The Neumayer station is situated on the Ekström Ice shelf at 70.7°S, 8.3°W, and the AWIPEV research base in the Kongsfjord at 78.9°N, 11.9°E. Both stations are close to the ocean, which is covered with sea ice during most of the year close to Neumayer. Kongsfjorden close to Ny Ålesund has usually remained ice-free throughout the winter in the last decade. We derive the DTR and daily average temperature from the original data provided with a frequency of 10 min.

2.2. Gridded Temperature Data

We use average temperature and the DTR from the CRU land temperature data set CRU TS v4 (Harris et al., 2020), a quality-controlled homogenized data set of monthly gridded data based on global station observations (Harris et al., 2014) of surface air temperature. We restrict our evaluation to grid points that include at least one station for interpolation throughout the entire timeframe considered.

2.3. CMIP6 Model Output

We use monthly means of daily maximum, daily minimum and average temperature (tasmax, tasmin, tas) for 1950–2014 from the historical runs of the 6th coupled model intercomparison project (CMIP6, Eyring et al., 2016). Each model's land-sea mask (sftlf) is used to select grid points with at least 90% land coverage. We analyzed all models for which the required data was available at the DKRZ ESGF node (see Table S1 in Supporting Information S1).

3. Results and Discussion

3.1. Temperature-Dependance and Seasonal Cycle of DTR

Binning the DTR observed at AWIPEV and the Neumayer station according to the daily average temperature (Figure 1a) shows that the DTR decreases with increasing average temperature between about −10 and 0°C. This effect it surprisingly consistent between the two stations. Especially the smallest DTR are lower at Neumayer than at AWIPEV, likely due to the much more homogeneous terrain and full year-round snowcover at Neumayer. Correlations between the DTR and relative humidity, sunshine duration, surface pressure and near-surface wind speeds in Ny Ålesund observations are substantially lower than those between DTR and average temperature both on daily (not shown) and monthly time scales (Figure S1 in Supporting Information S1). While we find no relevant correlation between sunshine duration and DTR on monthly timescales for an Arctic station, Zhong et al. (2023) show strong correlations between cloud cover and DTR on interannual timescales, particularly in mid-latitude regions.

The dependence of DTR on mean temperature can also be understood through the relationship between minimum and maximum temperature: For minimum temperatures colder than −10°C, maximum and minimum temperatures increase at a similar pace (Figure 1b). For minimum temperatures between −10 and around 0°C, maximum temperatures increase only about half as much as minimum temperatures. For minimum temperatures between 0 and 10°C, maximum temperatures increase by nearly 2°C for every °C increase in minimum temperatures.
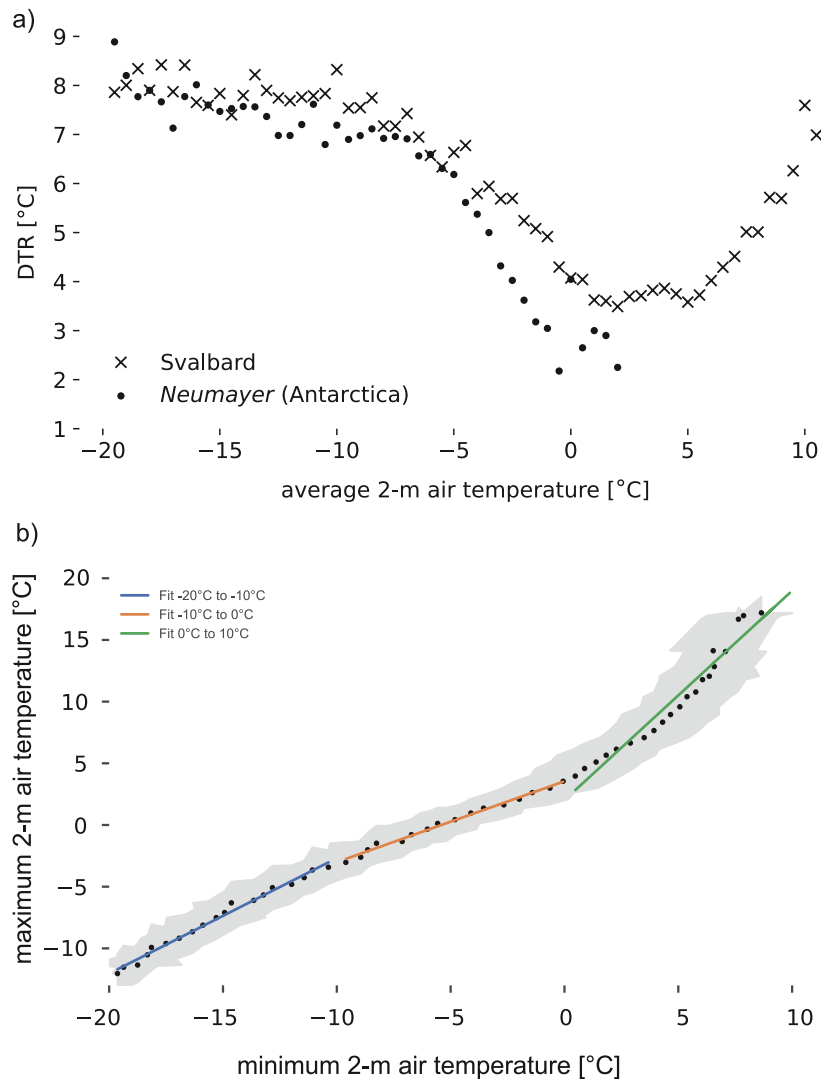
Figure 1. (a) DTR observed at AWIPEV (1994–2022) and Neumayer (1983–2022), binned according to average temperatures. (b) Mean daily minimum versus mean daily maximum temperatures for each average temperature bin, same database as in (a). The slopes of the regression lines are 0.94 for $T_{min} < -10°C$, 0.66 for $-10°C < T_{min} < 0°C$ and 1.7 for $0°C < T_{min} < 10°C$. Shading in (b) indicates a 70% confidence interval. Confidence intervals for figure (a) are given in Figure S1 of the Supporting Information S1.

Plotting each month's DTR against its mean temperature for the high-latitude land areas represented in the CRU data set (Figure 2) further supports the existence of a DTR minimum close to 0°C. The high-latitude DTR has a seasonal cycle that goes beyond the temperature-dependence, with spring showing a higher DTR than autumn for a similar average temperature. From September through February, mean temperature decreases and the DTR expands accordingly, but from February to April, the DTR continues to expand to its highest values while the average temperature also increases. The DTR then shrinks again with further increasing temperature until the mean temperature reaches 0°C in June, and DTR expands with mean temperature warming beyond 0°C in July and August.

We attribute this seasonal cycle to the presence of snow and a higher solar zenith angle during spring than autumn for comparable mean temperatures (Cerveny & Balling Jr, 1992). Snow has a low heat capacity and conductivity, which leads to a low effective heat capacity at the surface and thus a strong response of the surface temperature to imbalances in the surface energy budget, which contribute to a larger DTR. Higher maxima of solar radiation contribute to a larger diurnal cycle in the surface energy budget and thereby to a larger DTR.
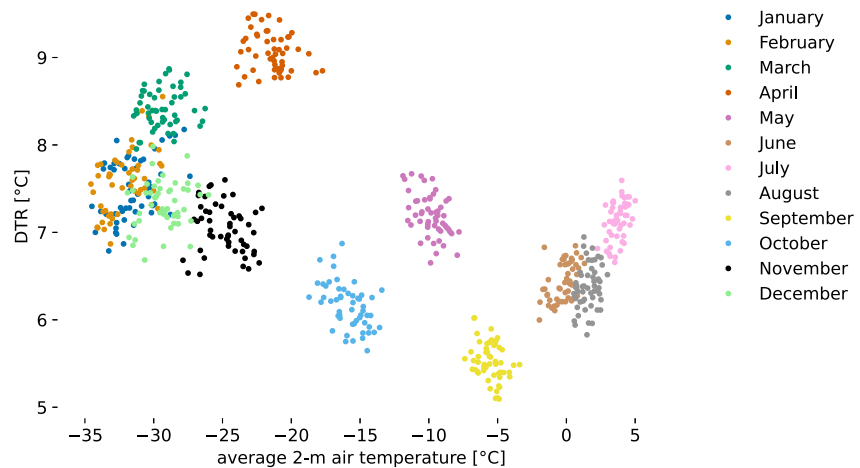
Figure 2. DTR for CRU data, binned according to average temperatures. Each point represents data from an individual month in the period 1970–2022 averaged over the land area between 70°N and 90°N.

3.2. The Melting-Point Effect

We attribute the effect of the freezing/melting point on DTR to the increased latency of surface temperature close to the phase change of water: When the surface is frozen and warms, it cannot easily warm beyond 0°C without first melting the frozen ground moisture or snowpack. When the surface temperature of bare soil is above the melting point and the surface cools, ground moisture needs to freeze, releasing latent heat, before the ground can cool below 0°C. In quantitative terms, when the melting point is not affected, the DTR for the surface temperature is a function of the diurnal cycle of the surface energy budget and the effective heat capacity of the surface.

$$DTR_{surf} = \frac{Q}{c_{eff}},$$ (1)

where Q is the surface energy flux integrated from minimum to maximum temperatures (or vice versa) and c_{eff} the effective heat capacity of the surface, governed by the surface material composition and the penetration depth of the diurnal cycle. When the temperature of the warming surface reaches 0°C, the latent heat of fusion for any existing snowpack and frozen moisture is taken up at the surface without further temperature changes. Only if all snow and soil moisture melt within a day, the soil continues to warm beyond 0°C,

$$DTR_{surf} = \frac{Q - Q_{melt}}{c_{eff}},$$ (2)

but the energy that was required to melt the snow/ice is no longer available to increase the surface temperature. An analogous argument can be made for a surface cooling to and below 0°C in the presence of soil moisture. The DTR of 2 m air temperature is not equal to the range or surface temperature, but closely coupled to the latter.

These constraints are usually effective on days with an average temperature between −10 and 10°C, as the typical range of diurnal temperature variability for such days encompasses 0°C. Across all months, about 30% of the land area covered by the CRU data set is in this temperature bracket. Virtually all extratropical land masses are in this temperature bracket from −10 to 10°C for at least part of the year (see Figure S2 in Supporting Information S1). We therefore expect the melting-point effect to be relevant for global mean DTR and its trend.

3.3. Seasonality and Temperature-Dependence of DTR Trends

If the relationship between DTR and average temperature shown in Figure 1 was the only mechanism causing DTR changes in a warming climate, we would expect DTR to shrink for average temperatures between −10 and 0°C, where warming shifts the average temperature toward the DTR minimum, and to expand for average temperatures between 0 and 10°C, where warming shifts the average temperature away from the DTR minimum.
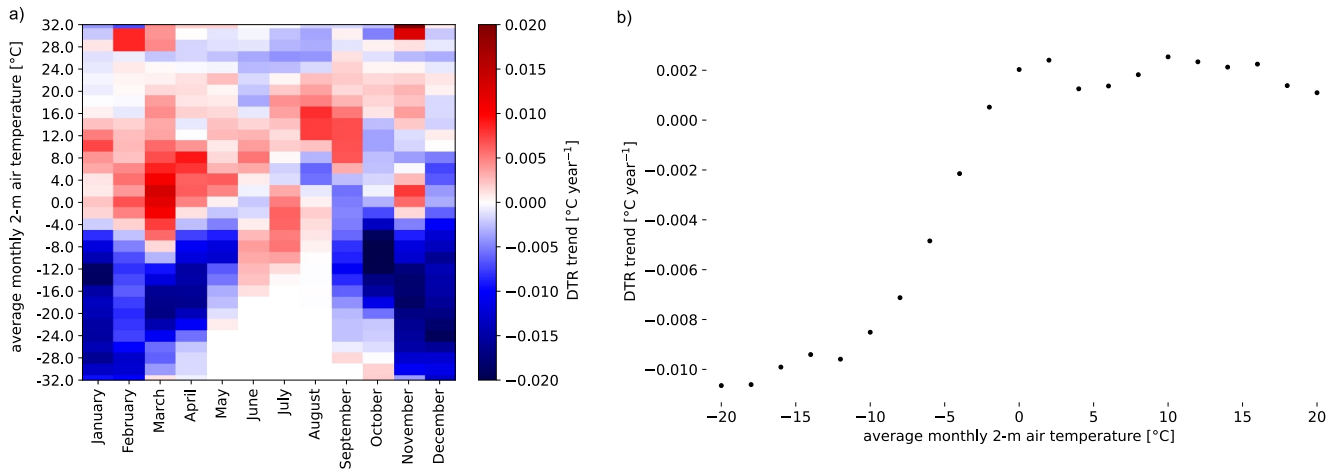
Figure 3. (a) DTR trends in the CRU data set (global land areas covered, 1970–2022) as a function of calendar month and mean temperature, (b) DTR trends binned as a function of monthly mean temperature.

Indeed, observed DTR over global land areas is mostly shrinking in months and places with an average temperature below 0°C, and expanding at warmer average temperature (Figure 3). This holds across seasons with some variance in the temperature threshold for positive/negative trends (Figure 3a). Binning trends according to average temperature (Figure 3b) shows the strongest DTR shrinking for negative average temperatures and DTR expansion for positive average temperatures.

The relationship between DTR and average temperature explains the observed relationship between DTR trends and the average temperature, but not the total observed DTR trends. It is not the major driver for shrinking DTR in response to global warming (Jackson & Forster, 2013), but it may have an important effect on regional, seasonal and (multi-)decadal differences in DTR trends.

In addition to the melting point effect on DTR, the maximum temperature during dry, hot summers increases more strongly than the average and minimum temperature because dry soils are no longer cooled by evaporation. This additional increase in maximum temperatures leads to an increase in DTR in areas affected by droughts (Daramola et al., 2024).

3.4. Temperature-Dependence of DTR and Its Trend in CMIP6 Models

Most CMIP6 models reproduce the observed relationship between DTR and mean temperature with a minimum DTR near the melting point (Figure 4). For further analyses, we separate models with no or a weak melting-point effect and thus DTR minimum near 0°C, marked by dashed lines in Figure 4. We use two criteria to assess the representation and strength of a melting-point effect in models, the difference in DTR between the local minimum and a local maximum at colder temperature, Δmin > 1°C, and the difference between the DTR at average temperatures of 0 versus 10°C, Δ(0 vs. 10) > 3°C (sketched in the inset in Figure 4). We consider models that fulfill both criteria as models with a melting point effect and models that do not fulfill either of the criteria as models with no or a weak melting point effect. Observations point toward a substantially larger Δmin, so our assessment of differences between these groups of models is a conservative estimate.

In most models, the difference between the DTR minimum and the DTR at lower and higher temperatures ranges from about 1°C to about 6°C. The EC-Earth models do not show the observed DTR minimum near the freezing/melting point despite including a parameterization of the effect of soil moisture freezing (Viterbo et al., 1999). The effect could be related to other schemes, such as the representation of the snowpack, or it could be too weak in the EC-Earth models due to issues in atmosphere-surface coupling or in the soil moisture freezing scheme itself. The GISS models only fulfill the second (Δ(0 vs. 10)) criterion and are not considered part of either subgroup of models.

The DTR itself also has a strong inter-model spread, ranging from 4 to 10°C for an average temperature of 0°C when excluding the outlier model AWI-CM-1-1-MR with a DTR around 20°C. While a full evaluation of the
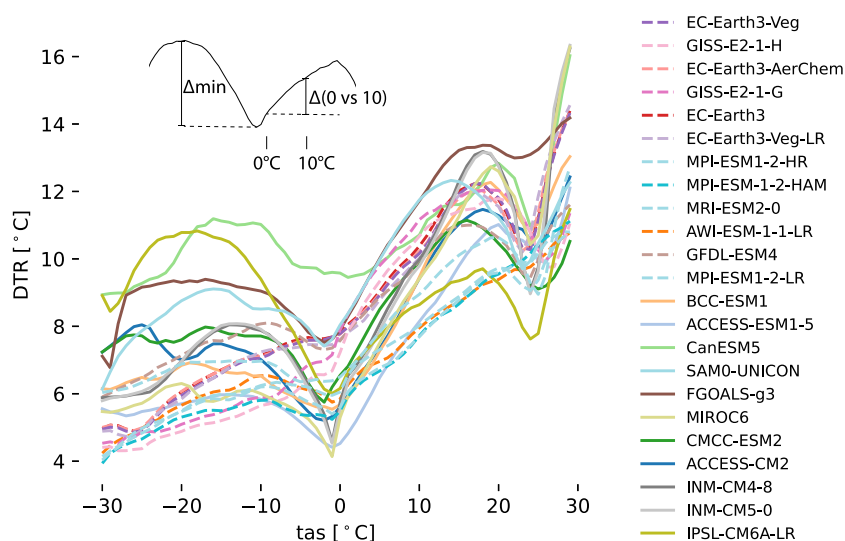
Figure 4. DTR as a function of monthly mean surface air temperature (tas) in CMIP6 climate models (historical run, global land areas, 1950–2014). Models are sorted by Δmin, and dashed lines show models with a particularly weak representation of melting-point effect on DTR (Δmin < 1°C). The inset sketches the definition of both criteria used to determine the existence and strength of a melting-point effect in models, the strength of the local DTR minimum relative to the maximum DTR at colder temperature Δmin and the difference in DTR at an average temperature of 10 versus 0°, Δ 0 versus 10.

DTR in climate models is beyond the scope of this paper, our high-latitude observations indicate typical DTR around 8°C for average temperatures below −10°C. This would be on the upper end of the CMIP6 inter-model spread at similar average temperature, consistent with earlier findings that CMIP5 climate models tend to underestimate DTR (Lindvall & Svensson, 2015).

For surface air temperatures above the local minimum near 0°C, climate models agree on a general expansion of DTR with increasing temperature, with a second local minimum near 25°C. This might seem at odds with a general trend of shrinking DTR with global warming, but the effect of anthropogenic climate change on DTR partly occurs as a rapid adjustment, that is, a direct response to the increased greenhouse gas concentration and its radiative effects that is independent of surface temperature change (Jackson & Forster, 2013). The response of DTR to climate change thus cannot be expected to follow the temperature-DTR relationship in a given climate state.

Computing global DTR trends for models with no or a weak representation of the melting-point effect on DTR separately from models with a substantial melting-point effect (Figure 5) shows that the latter display a significantly (p = 0.002 for a one-sided Welch *t*-test) weaker DTR shrinking after than prior to 1985. In models with a weak or no melting-point effect, the DTR continues shrinking with no significant difference between the earlier and later period.

Models reproduce observations of substantial shrinking of the DTR at average temperature below 0°C, and weaker shrinking or expansion of the DTR for temperatures around 10°C (observations in Figure 3b, models in Figure S2 of the Supporting Information S1). Models with a meting-point effect have a near-zero DTR trend for an average temperature around 10°C between 1970 and 2014.

Models with no or a weak melting-point effect project stronger DTR shrinking throughout the 21st century than models with a substantial melting point effect, as well as a stronger DTR change normalized by global mean surface temperature change (not shown).

4. Conclusions

The DTR strongly depends on average temperatures in the (average) temperature range from −10 to 10°C, with a minimum DTR near 0°C and larger DTR for both warmer and colder temperatures. We attribute this to a melting-point effect, where latent heat release or uptake during the freezing/melting of water limits the DTR when
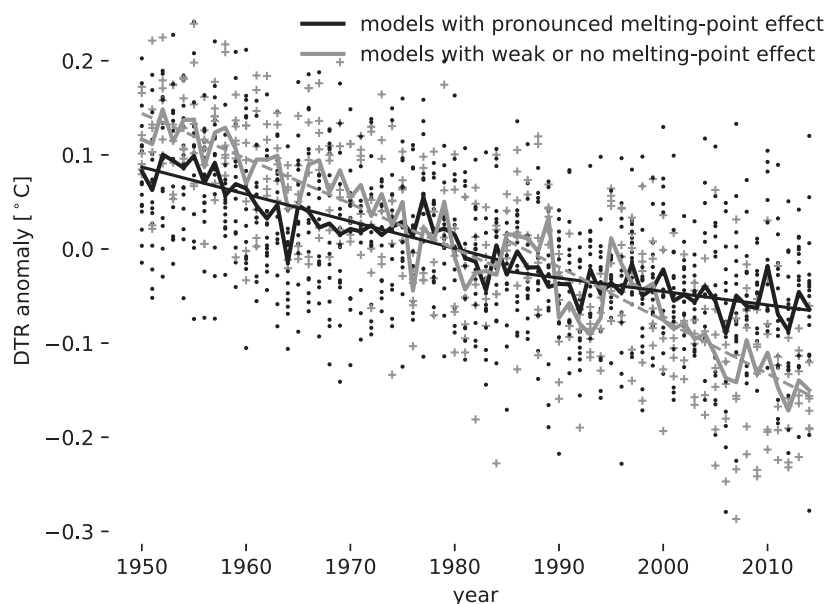
Figure 5. Annual mean DTR anomaly with respect to 1950–2014 in CMIP6 climate models (historical run) over global land areas and linear trends before and after 1985. Dots/plus signs represent individual models, and lines the mean over models with a substantial DTR minimum near 0°C (black, dots) or a weak or no DTR minimum (gray, plus signs, corresponding to models shown with dashed lines in Figure 4).

temperatures approach 0°C. For temperatures below −10°C and above 10°C, climate models indicate mostly larger DTR with larger average temperatures and a second minimum for average temperatures above 25°C.

The relationship between DTR and average temperature is not the major driver for shrinking DTR in response to global warming (Jackson & Forster, 2013), but it affects global DTR trends on decadal to multidecadal time scales and their seasonal and geographical distribution. Observed DTR trends in recent decades are predominantly shrinking for average temperatures below 0°C and expanding for average temperatures above 0°C, consistent with the melting-point effect on DTR. In addition to the melting-point effect, land-surface feedbacks due to drying and reduced evaporation in summer contribute to positive trends at warmer temperature (Daramola et al., 2024).

Climate models that represent the minimum DTR near average temperatures of 0°C show a weaker shrinking of global-mean DTR between 1985 and 2014 than prior to 1985, whereas models that (largely) lack this minimum simulate a steadily shrinking DTR. The DTR trend in models that represent the melting-point effect on DTR is thus more consistent with observations suggesting a recent growth in DTR (Huang et al., 2023).

The lack of a DTR minimum near 0°C in some models points to issues in atmosphere-surface coupling that should be further investigated. The substantial inter-model spread in DTR (on the order of 5°C for a given average temperature) could also be leveraged to evaluate atmosphere-surface coupling in models. We further suggest to investigate the mechanisms behind the second minimum in DTR above 25°C and compare this feature in models to observations from lower latitudes.

Data Availability Statement

References

Braganza, K., Karoly, D. J., & Arblaster, J. M. (2004). Diurnal temperature range as an index of global climate change during the twentieth century. *Geophysical Research Letters*, *31*(13), L13217. https://doi.org/10.1029/2004gl019998

Cerveny, R. S., & Balling Jr, R. C. (1992). The impact of snow cover on diurnal temperature range. *Geophysical Research Letters*, *19*(8), 797–800. https://doi.org/10.1029/92gl00573

Cheng, J., Xu, Z., Zhu, R., Wang, X., Jin, L., Song, J., & Su, H. (2014). Impact of diurnal temperature range on human health: A systematic review. *International Journal of Biometeorology*, *58*(9), 2011–2024. https://doi.org/10.1007/s00484-014-0797-5

Dai, A., Genio, A. D. D., & Fung, I. Y. (1997). Clouds, precipitation and temperature range. *Nature*, *386*(6626), 665–666. https://doi.org/10.1038/386665b0

Dai, A., Trenberth, K. E., & Karl, T. R. (1999). Effects of clouds, soil moisture, precipitation, and water vapor on diurnal temperature range. *Journal of Climate*, *12*(8), 2451–2473. https://doi.org/10.1175/1520-0442(1999)012<2451:eocsmp>2.0.co;2

Daramola, M. T., Li, R., & Xu, M. (2024). Increased diurnal temperature range in global drylands in more recent decades. *International Journal of Climatology*, *44*(2), 521–533. https://doi.org/10.1002/joc.8341

Doan, Q.-V., Chen, F., Asano, Y., Gu, Y., Nishi, A., Kusaka, H., & Niyogi, D. (2022). Causes for asymmetric warming of sub-diurnal temperature responding to global warming. *Geophysical Research Letters*, *49*(20), e2022GL100029. https://doi.org/10.1029/2022gl100029

Eyring, V., Bony, S., Meehl, G. A., Senior, C. A., Stevens, B., Stouffer, R. J., & Taylor, K. E. (2016). Overview of the coupled model inter-comparison project phase 6 (CMIP6) experimental design and organization. *Geoscientific Model Development*, *9*(5), 1937–1958. https://doi.org/10.5194/gmd-9-1937-2016

Gulev, S., Thorne, P., Ahn, J., Dentener, F., Domingues, C., Gerland, S., et al. (2021). Changing state of the climate system [Book Section]. In V. Masson-Delmotte, P. Zhai, A. Pirani, S. L. Connors, C. Péan, S. Berger, et al. (Eds.), *Climate change 2021: The physical science basis. Contribution of working group I to the sixth assessment report of the intergovernmental panel on climate change* (pp. 287–422). Cambridge University Press. https://doi.org/10.1017/9781009157896.004

Harris, I, Jones, P. D., Osborn, T. J., & Lister, D. H. (2014). Updated high-resolution grids of monthly climatic observations–the CRU TS3. 10. *International Journal of Climatology*, *34*(3), 623–642. https://doi.org/10.1002/joc.3711

Harris, I., Osborn, T. J., Jones, P., & Lister, D. (2020). Version 4 of the CRU TS monthly high-resolution gridded multivariate climate [Dataset]. *Scientific Data*, *7*(1), 109. https://doi.org/10.1038/s41597-020-0453-3

Huang, X., Dunn, R. J., Li, L. Z., McVicar, T. R., Azorin-Molina, C., & Zeng, Z. (2023). Increasing global terrestrial diurnal temperature range for 1980–2021. *Geophysical Research Letters*, *50*(11), e2023GL103503. https://doi.org/10.1029/2023gl103503

Jackson, L. S., & Forster, P. M. (2013). Modeled rapid adjustments in diurnal temperature range response to CO_2 and solar forcings. *Journal of Geophysical Research: Atmospheres*, *118*(5), 2229–2240. https://doi.org/10.1002/jgrd.50243

Lindvall, J., & Svensson, G. (2015). The diurnal temperature range in the CMIP5 models. *Climate Dynamics*, *44*(1–2), 405–421. https://doi.org/10.1007/s00382-014-2144-2

Lobell, D. B. (2007). Changes in diurnal temperature range and national cereal yields. *Agricultural and Forest Meteorology*, *145*(3–4), 229–238. https://doi.org/10.1016/j.agrformet.2007.05.002

Maturilli, M. (2020). Continuous meteorological observations at station Ny-Ålesund (2011-08 et seq) [Dataset]. *Alfred Wegener Institute—Research Unit Potsdam, PANGAEA. PANGAEA*. https://doi.org/10.1594/PANGAEA.914979

Schmithüsen, H. (2023). Continuous meteorological observations at Neumayer station (1982-03 et seq) [Dataset]. *Alfred Wegener Institute, Helmholtz Centre for Polar and Marine Research, Bremerhaven, PANGAEA. PANGAEA*. https://doi.org/10.1594/PANGAEA.962313

Schwarz, M., Folini, D., Yang, S., Allan, R. P., & Wild, M. (2020). Changes in atmospheric shortwave absorption as important driver of dimming and brightening. *Nature Geoscience*, *13*(2), 110–115. https://doi.org/10.1038/s41561-019-0528-y

Stone, D., & Weaver, A. (2003). Factors contributing to diurnal temperature range trends in twentieth and twenty-first century simulations of the CCCma coupled model. *Climate Dynamics*, *20*(5), 435–445. https://doi.org/10.1007/s00382-002-0288-y

Viterbo, P., Beljaars, A., Mahfouf, J.-F., & Teixeira, J. (1999). The representation of soil moisture freezing and its impact on the stable boundary layer. *Quarterly Journal of the Royal Meteorological Society*, *125*(559), 2401–2426. https://doi.org/10.1002/qj.49712555904

Walters, J. T., McNider, R. T., Shi, X., Norris, W. B., & Christy, J. R. (2007). Positive surface temperature feedback in the stable nocturnal boundary layer. *Geophysical Research Letters*, *34*(12), L12709. https://doi.org/10.1029/2007gl029505

Wang, S., Zhang, M., Tang, J., Yan, X., Fu, C., & Wang, S. (2024). Interannual variability of diurnal temperature range in CMIP6 projections and the connection with large-scale circulation. *Climate Dynamics*, *62*(5), 1–16. https://doi.org/10.1007/s00382-024-07107-3

Wesche, C., Weller, R., König-Langlo, G., Fromm, T., Eckstaller, A., Nixdorf, U., & Kohlberg, E. (2016). Neumayer III and Kohnen station in Antarctica operated by the Alfred Wegener institute. *Journal of Large-Scale Research Facilities JLSRF*, *2*, A85. https://doi.org/10.17815/jlsrf-2-152

Zhong, Z., He, B., Chen, H. W., Chen, D., Zhou, T., Dong, W., et al. (2023). Reversed asymmetric warming of sub-diurnal temperature over land during recent decades. *Nature Communications*, *14*(1), 7189. https://doi.org/10.1038/s41467-023-43007-6

Zhou, L., Dai, A., Dai, Y., Vose, R. S., Zou, C.-Z., Tian, Y., & Chen, H. (2009). Spatial dependence of diurnal temperature range trends on precipitation from 1950 to 2004. *Climate Dynamics*, *32*(2–3), 429–440. https://doi.org/10.1007/s00382-008-0387-5

Erratum

The originally published version of this article contained an error in Figure 3a. The y-axis should read as follows: "Average monthly 2-m air temperature." The error has been corrected, and this may be considered the authoritative version of record.